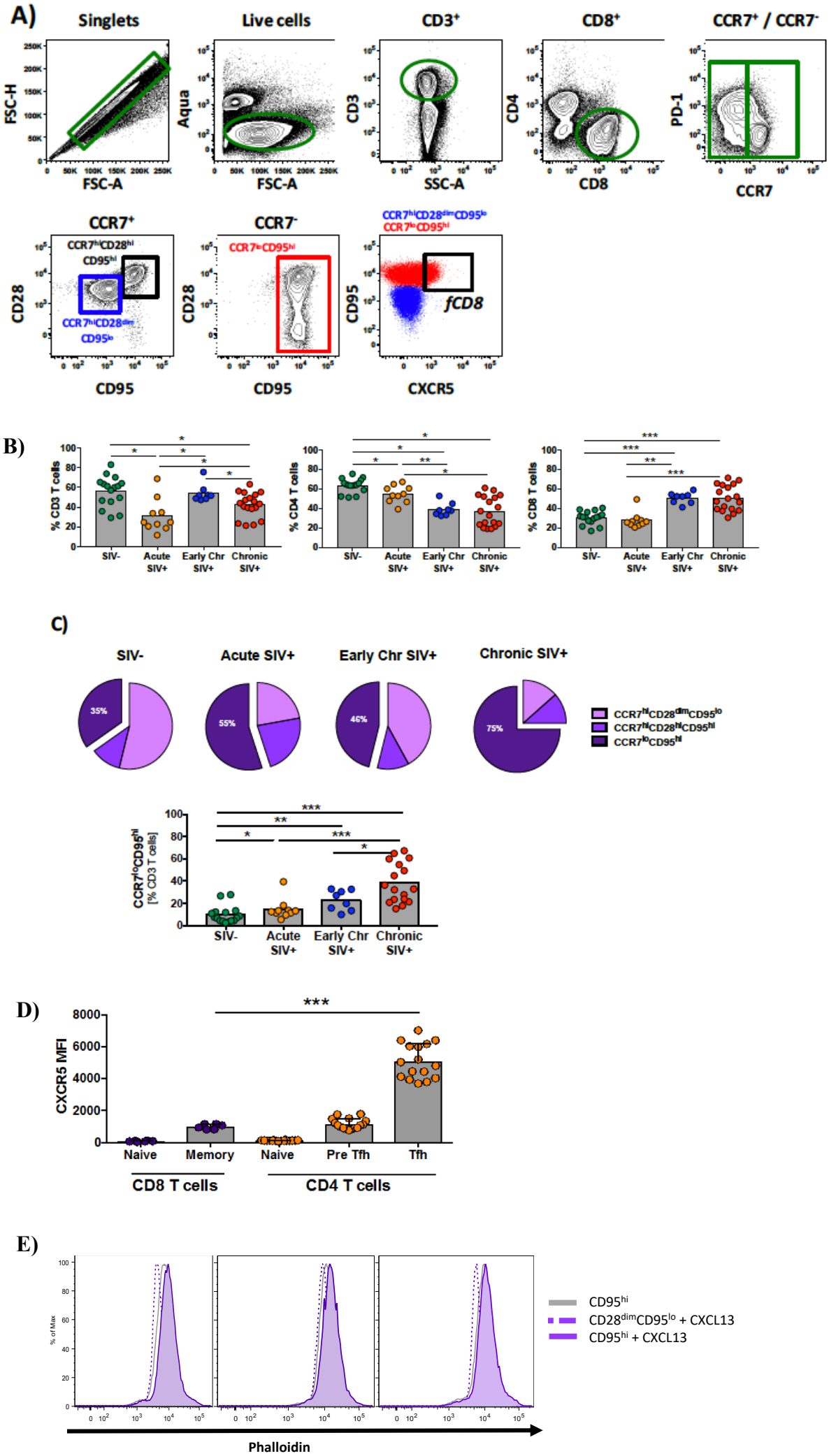

Figure S1. (A) Gating strategy for the CD8 T cell phenotype analysis. **(B)** Pooled data showing the relative frequency of total CD3, CD4 and CD8 T cells in LNs from non-infected (SIV-), acute (d14), early chronic (d45) and chronic (> 6 months) SIV infected RMs. **(C)** The relative appearance of LN CD8 T cell subsets (*upper panel*) and frequency of LN CCR7^{lo}CD95^{hi} CD8 T cells (*lower panel*) in SIV-, acute and chronically SIV infected RMs. **(D)** Expression of CXCR5 per cell, judged by Mean Fluoresense Intensity-MFI, on LN CD4 and CD8 subsets from chronically SIV infected RMs. **(E)** Histograms depicting the F-actin mobilization, judged by phalloidin increase, in LN naïve (CD28^{dim}CD95^{lo}) and memory CD95^{hi} CD8 T cells from 3 chronically infected RMs after short (5 sec) *ex vivo* stimulation with CXCL10. *p < 0.05; ** < 0.001; ***p < 0.0001. Mann-Whitney U test for unpaired comparisons.

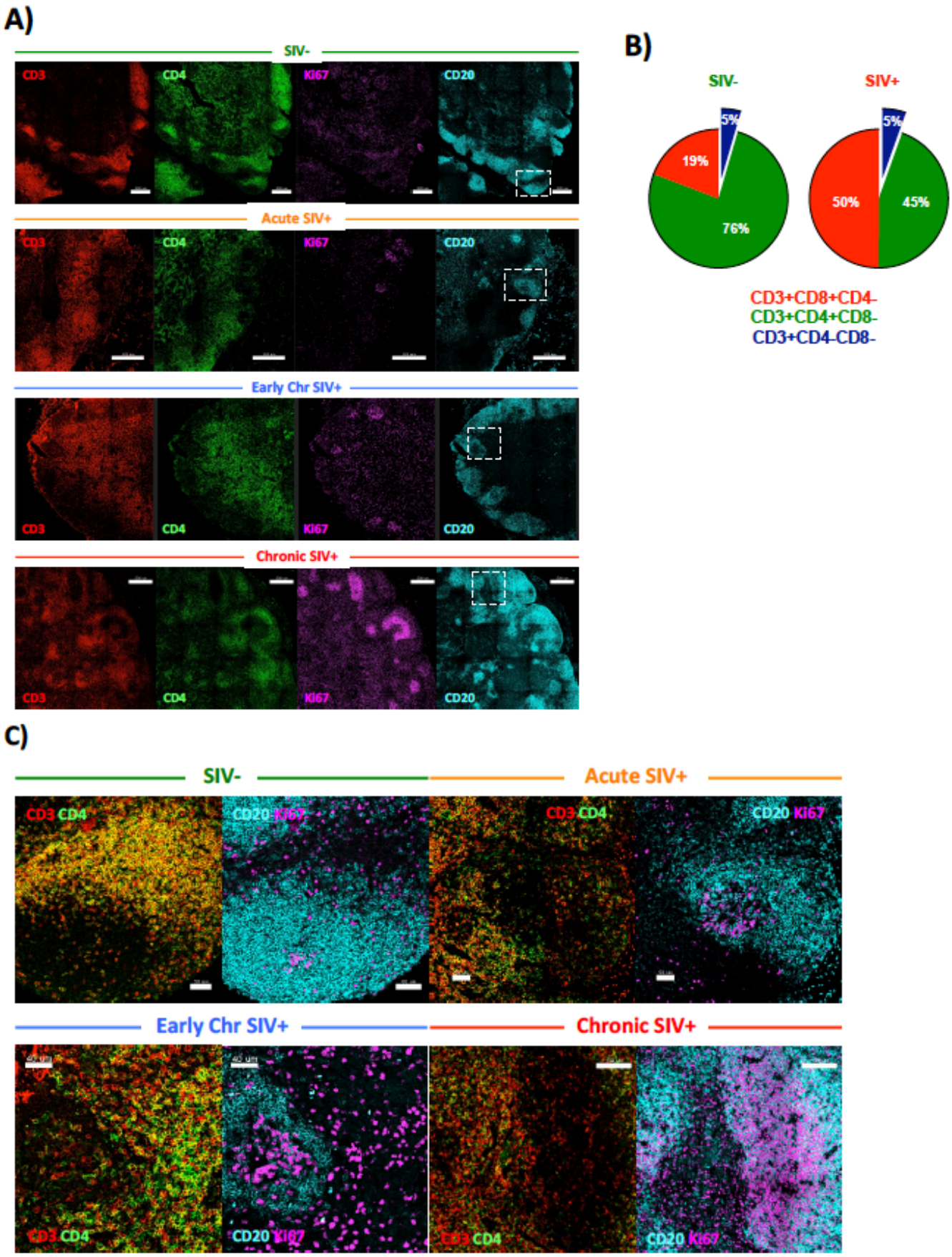

Figure S2. (A) Representative confocal images (20X) showing the staining with anti-CD3, anti-CD4, anti-Ki67 and anti-CD20 antibodies of a non-infected (SIV-), acute (d14), early chronic (d45) and chronic (> 6 months) SIV-infected RM LN. **(B)** Relative appearance of CD3+CD4-CD8- T cells in SIV- and chronically SIV infected RM LNs. **(C)** Representative confocal images (20X) showing the CD4 (CD3+CD4+) and CD8 (CD3+CD4-) T cell distribution in non-infected (SIV-), acute (d14), early chronic (d45) and chronic (> 6 months) SIV-infected LN. CD3/CD4 and CD20/Ki67 merged images are shown. Zoomed images correspond to the highlighted areas (white boxes) in section (A).

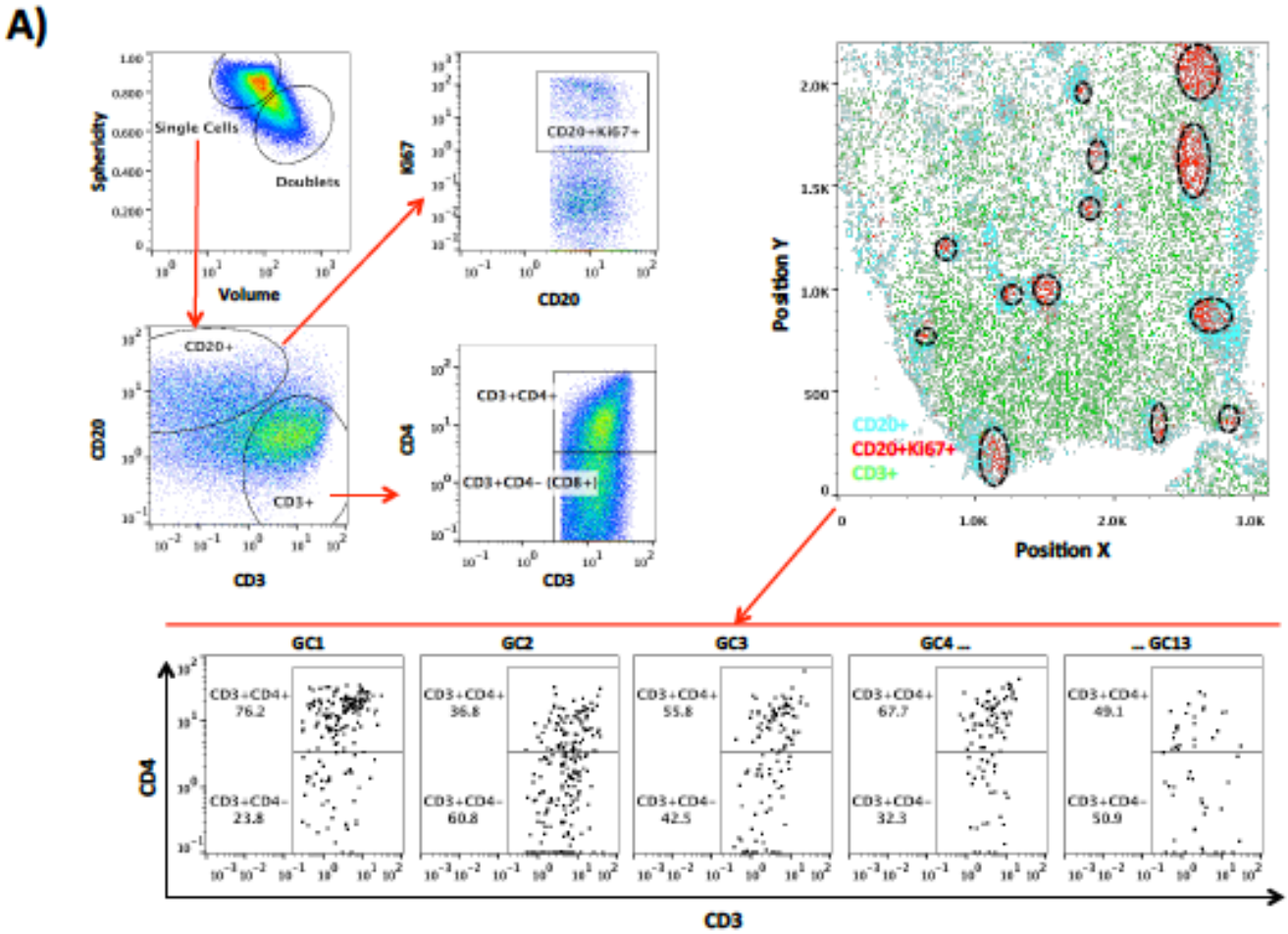

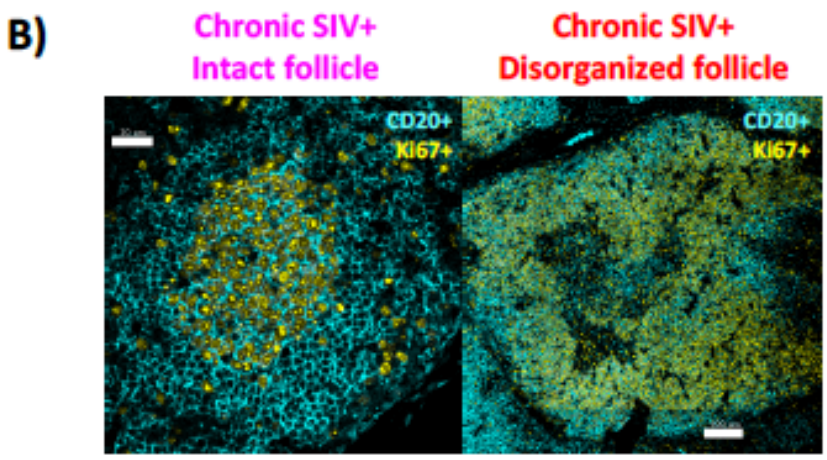

Figure S3. (A) Representative example of the Histo-cytometry gating strategy. Analysis from a chronic SIV infected LN is shown. The relative frequency of $CD3^{+}CD4^{+}$ and $CD3^{+}CD4^{-}$ cells in different follicles (n=5) is also shown. **(B)** Representative confocal images (40X) of intact and disorganized follicles/germinal centers in a chronically SIV infected RM.

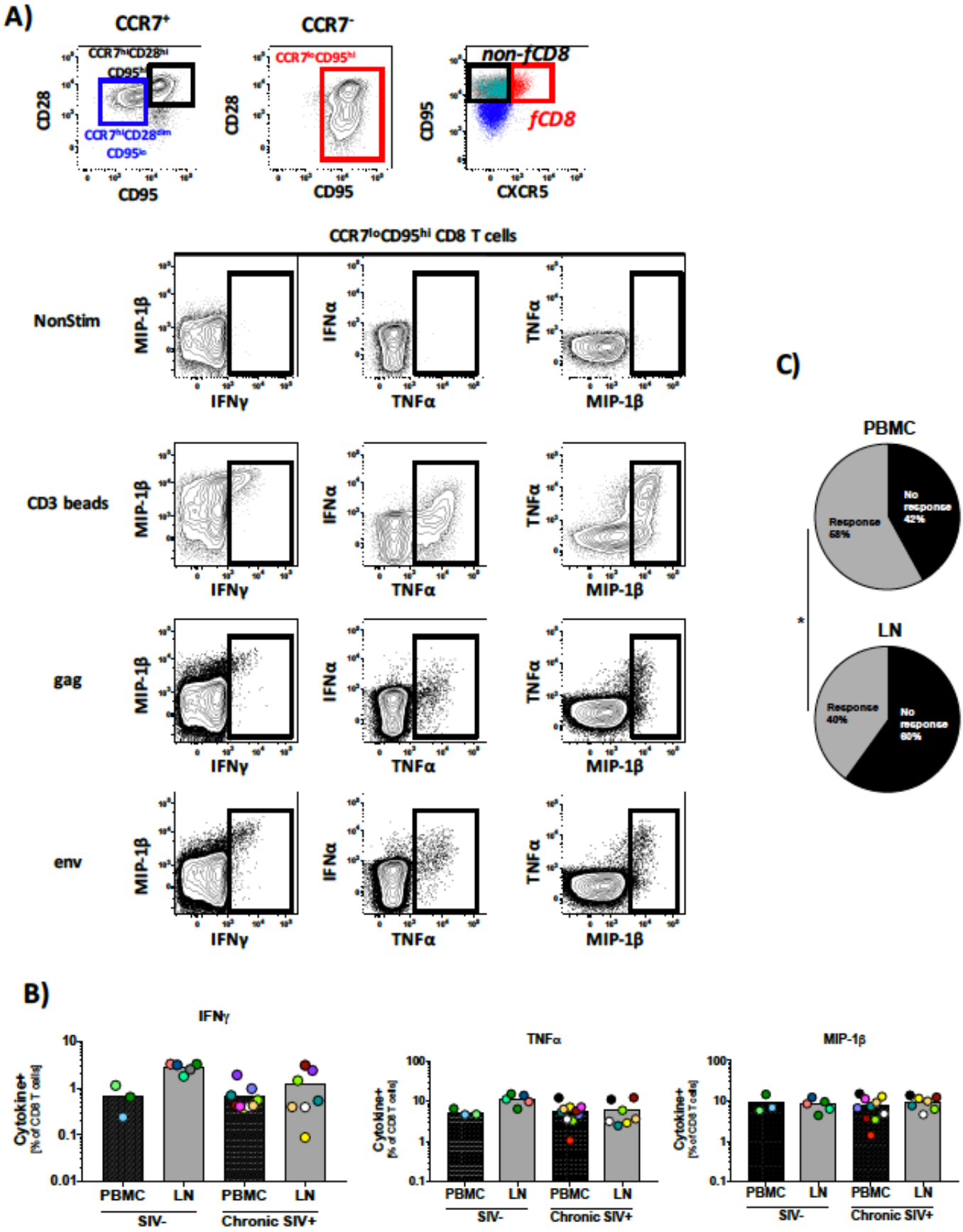

Figure S4. (A) Gating strategy showing the analysis of either general TCR (anti-CD3 stimulation) or antigen-specific (Gag and Env stimulation) CCR7^{lo}CD95^{hi} CD8 T cells. **(B)** Pooled data showing the IFNγ, TNFα and MIP-1β production after short-term (6h) stimulation with anti-CD3 beads in LN and PBMC populations. Results are showed as frequency of total CD8 T cells. **(C)** Frequency of paired PBMC and LN samples responding to Gag and/or Env stimulation. Matching samples are highlighted with paired colors. *$p < 0.05$. Mann-Whitney U test for unpaired comparisons.

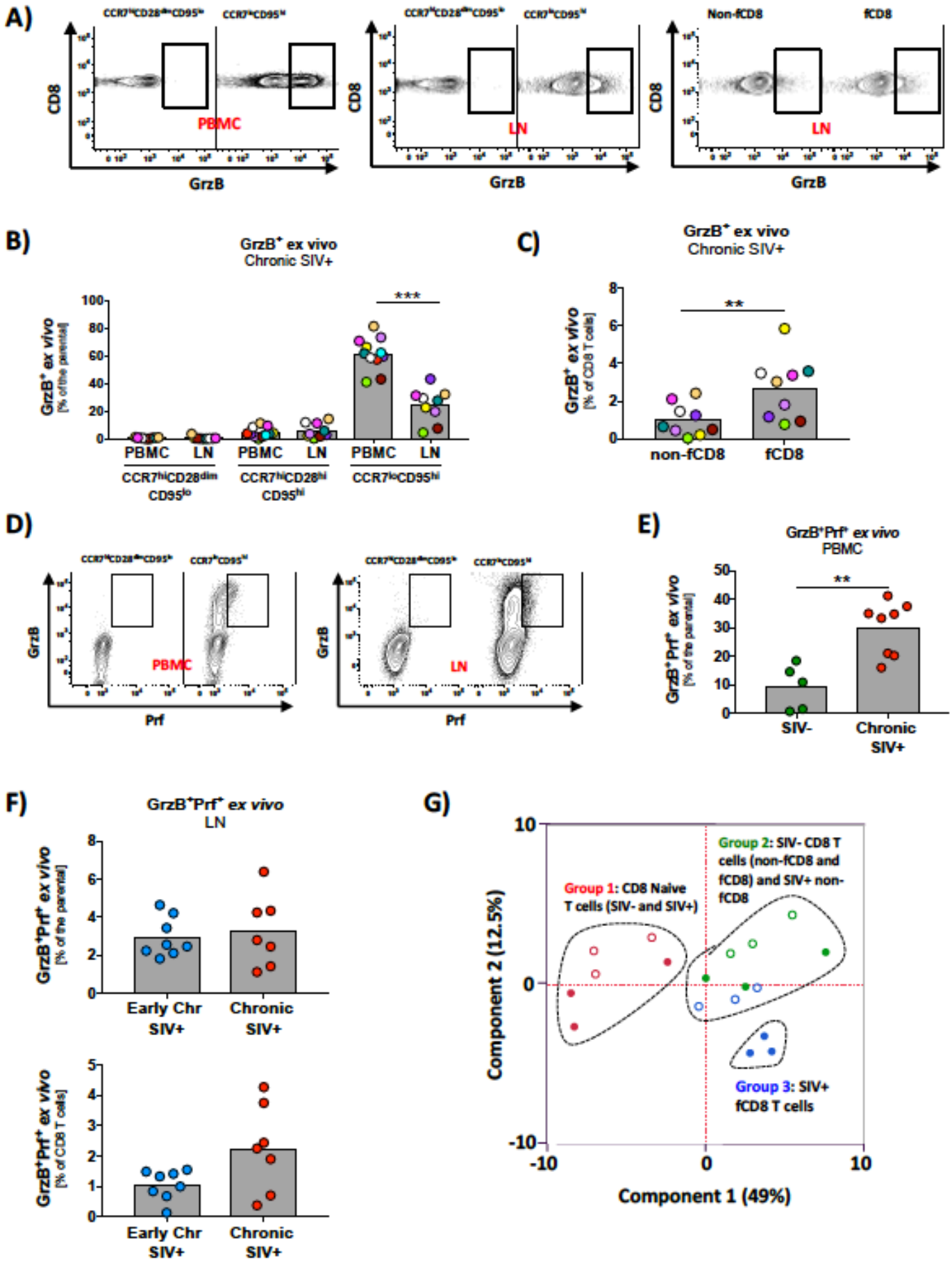

Figure S5. (A) Gating strategy for *ex vivo* GrzB quantification. Pooled data showing the frequency of GrzB$^+$ cells in PBMC and LN CD8 T cell subsets **(B)** and non-fCD8 and fCD8 T cells from chronically SIV infected RM LNs **(C)**. **p< 0.001; ***p < 0.0001. **(D)** Gating strategy for *ex vivo* GrzB and Prf quantification. Pooled data showing the GrzB$^+$Prf$^+$ *ex vivo* expression in CCR7^{lo}CD95^{hi} CD8 T cells from uninfected and chronically SIV infected RM PBMC samples **(E)** and early (d45) and late (> 6 months) chronically SIV infected RM LNs **(F)**. Results are shown as frequency of the parental (*upper panel*) and frequency of total CD8 T cells (*lower panel*). **p < 0.001. **(G)** Principal component analysis (PCA) of two components (CD8 subset and SIV infection) showing the results of the Fluidigm analysis. Different colors represent different CD8 T cell subsets. CCR7^{hi}CD28^{dim}CD95^{lo} red; non-fCD8 green; fCD8 blue. SIV$^-$ open circles, SIV$^+$ ted with paired colors. Mann-Whitney U test for unpaired comparisons.

A)

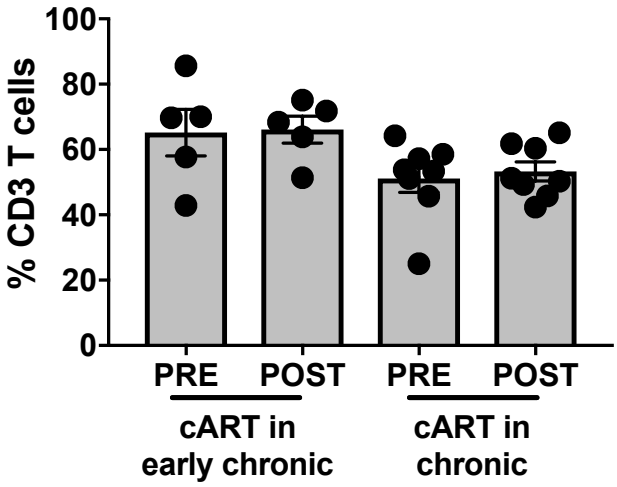

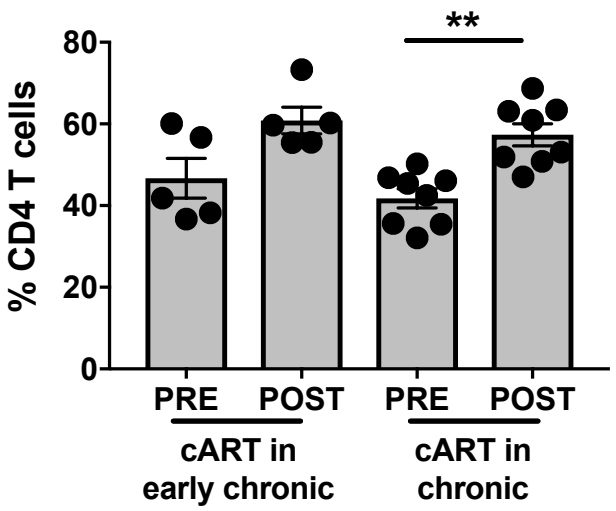

Figure S6. (A) Pooled data showing the relative frequency of LN total CD3 and CD4 T cells pre- and post-cART from RMs treated during early (n=5) or late (n=8) chronic SIV infection. Wilcoxon test for unpaired comparisons.

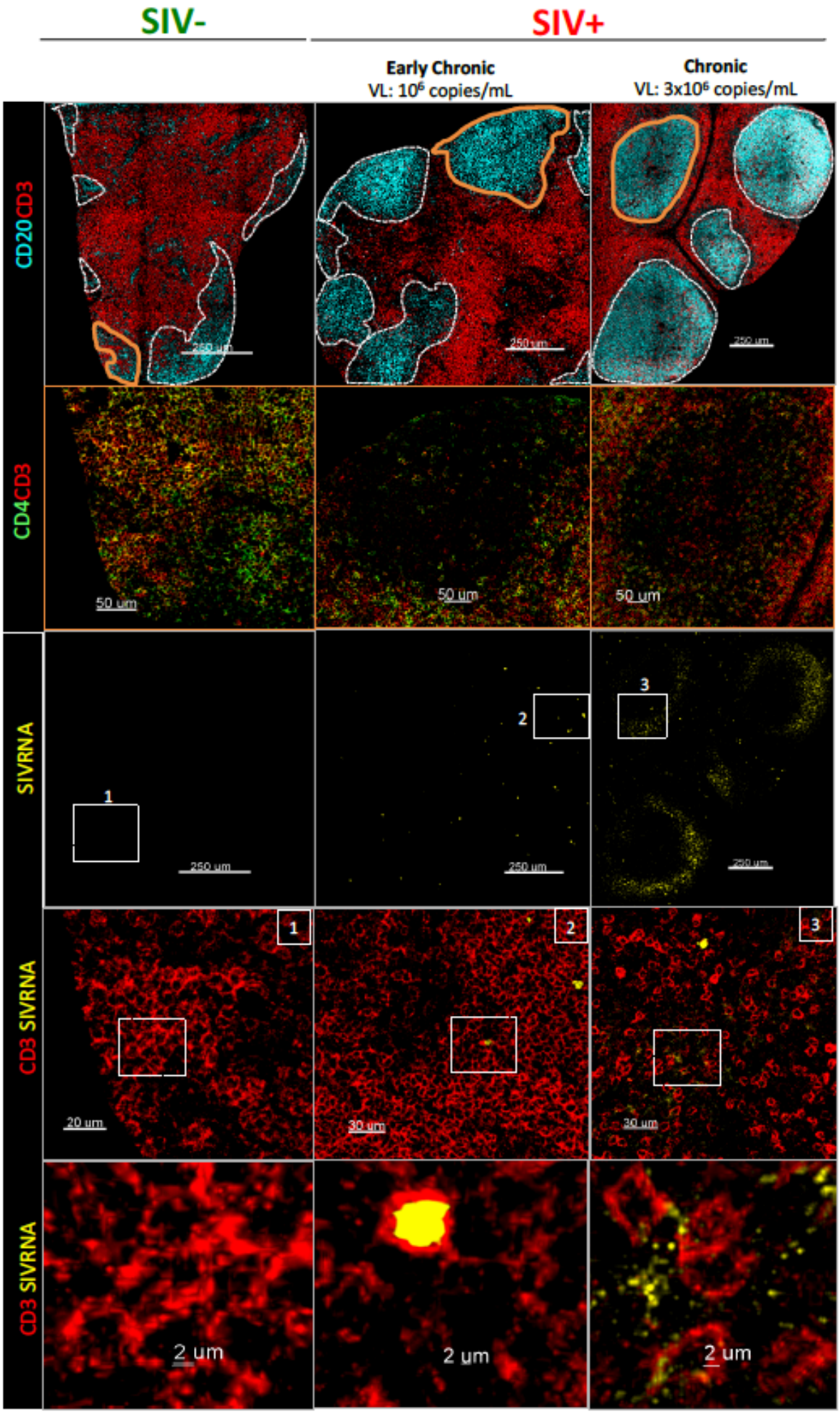

Figure S7. Representative confocal images (40X) of FFPE tissue sections stained with SIV RNA probes using in-situ hybridization protocol (RNAscope) for visualization of viral RNA. Non-infected (SIV-), early (d45) and late (> 6months) chronically SIV infected RM LN are shown. CD20/CD3, CD4/CD3 and CD3/SIV RNA merged images are shown together with zoomed images (bottom row) from the highlighted areas (white squares).

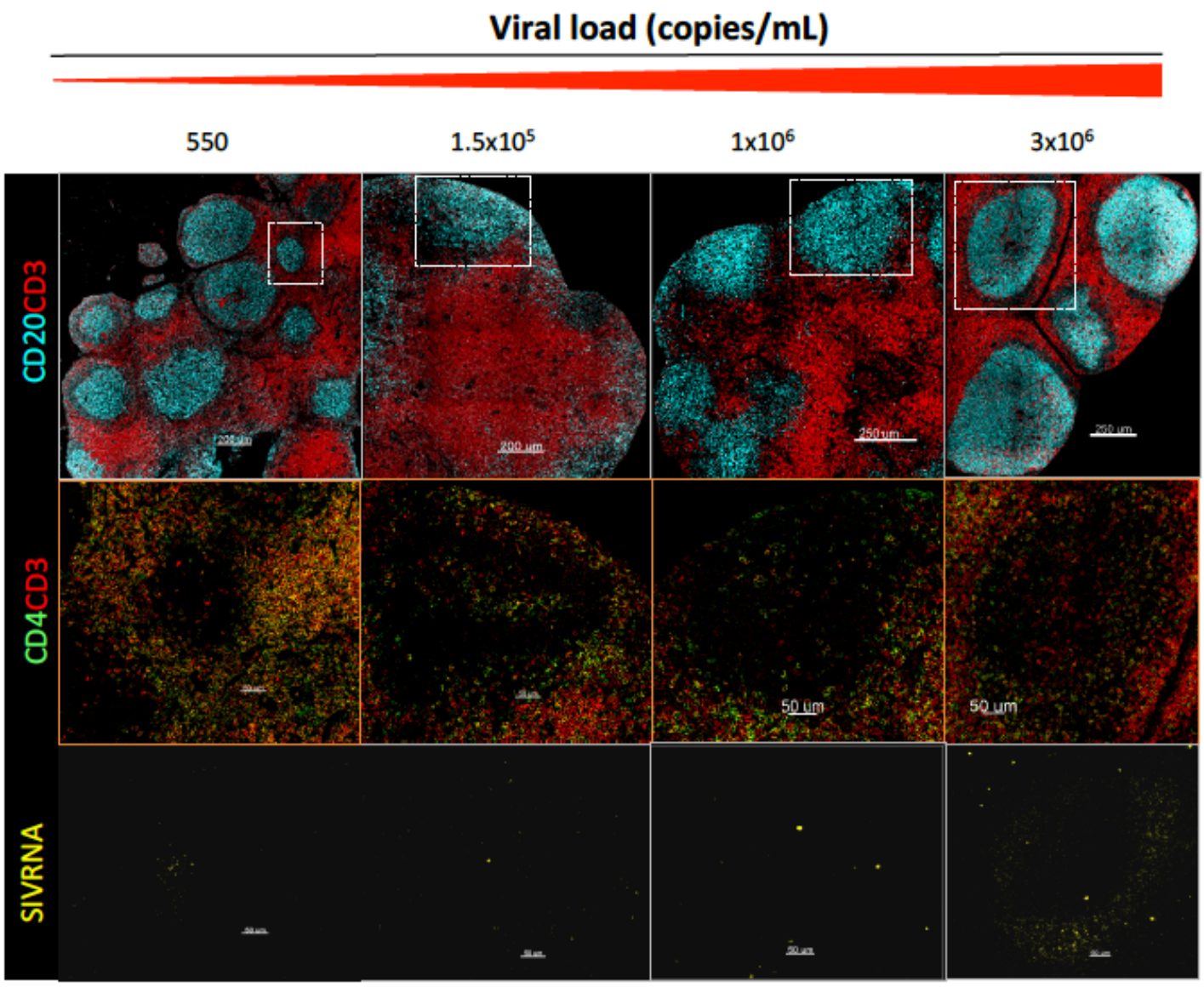

Figure S8. Representative confocal images (40X) of FFPE tissue sections stained with SIV RNA probes using in-situ hybridization protocol (RNAscope) for visualization of viral RNA. SIV-infected LN with different viral loads (RNA copies/mL) are shown. Zoomed images (central and bottom rows) from the highlighted areas (white squares) are shown. Areas shown in S7 for the $1x10^6$ and $3x10^6$ VL tissues are presented here too.

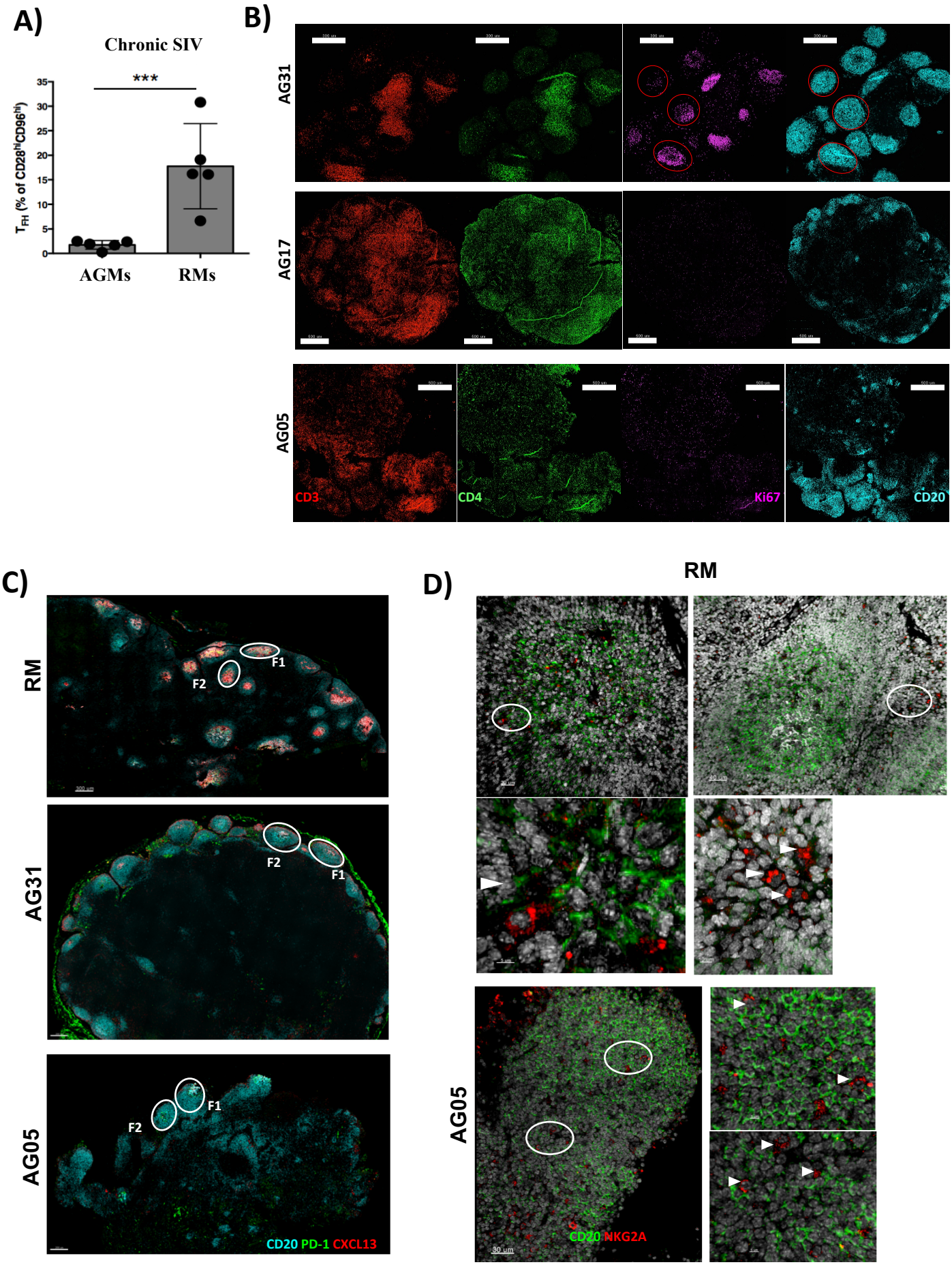

Figure S9. (A) Pooled data showing the relative frequency of T_{FH} CD4 T cells in chronically SIV infected RMs (n=5) and AGMs (n=5). ***p<0.001. **(B)** Representative confocal images of LN tissue sections from chronic SIV infected AGMs stained with CD3 (red), CD4 (green), Ki67 (magenta) and CD20 (cyan). **(C)** Confocal images of LN tissue sections from chronic SIV infected RM and two AGMs stained for CD20 (cyan), PD-1 (green) and CXCL13 (red) are shown. Two zoomed follicular areas (white circle) from each animal are shown in the Figure 5G. **(D)** Confocal images showing the staining for CD20 (green) and NKG2A (red) in a LN from a chronically SIV infected RM (upper panel) and AGM (lower panel). A zoomed (white circle) follicular and an extra-follicular area from each animal is also shown. White arrows point to NKG2A positive cells.

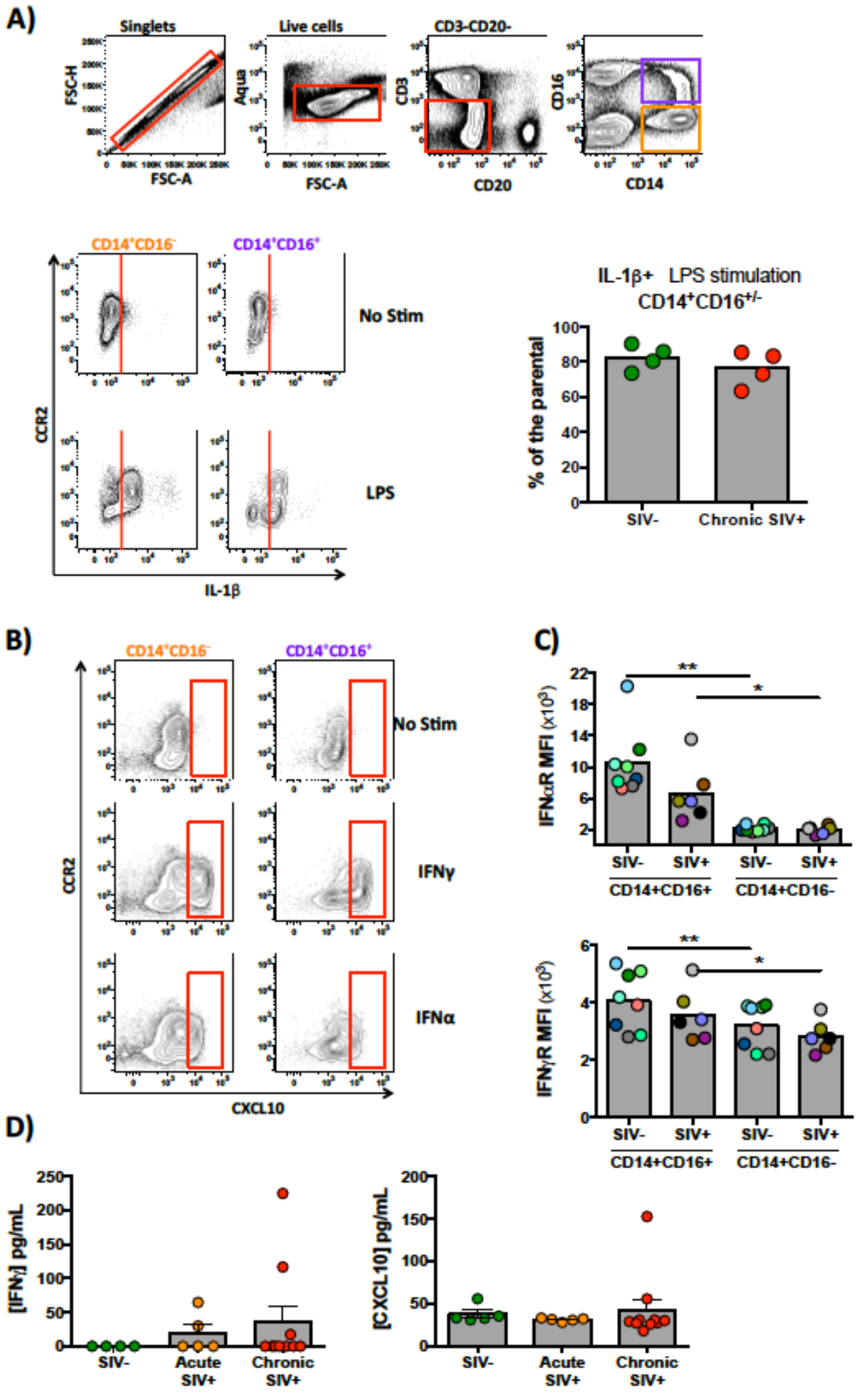

Figure S10. (A) Gating strategy for the identification of monocyte populations (*upper panel*). Gating scheme and pooled data showing the IL-1β production by blood monocytes from non-infected and chronically SIV infected RMs after *ex vivo* stimulation with LPS. Results are shown as frequency of the parental population. **(B)** Gating strategy for the analysis of CXCL13 production after IFN stimulation. **(C)** Pooled data showing the expression of INFαR and IFNγR per cell (MFI) among monocyte subsets from non-infected and chronically SIV infected RMs. *$p < 0.05$; **$p < 0.001$. **(D)** Levels of circulating IFNγ and CXCL10 in non-infected, acute (d14) and chronic (> 6 months) SIV infected RMs. Matching samples are highlighted with paired colors. Mann-Whitney U test for unpaired comparisons.

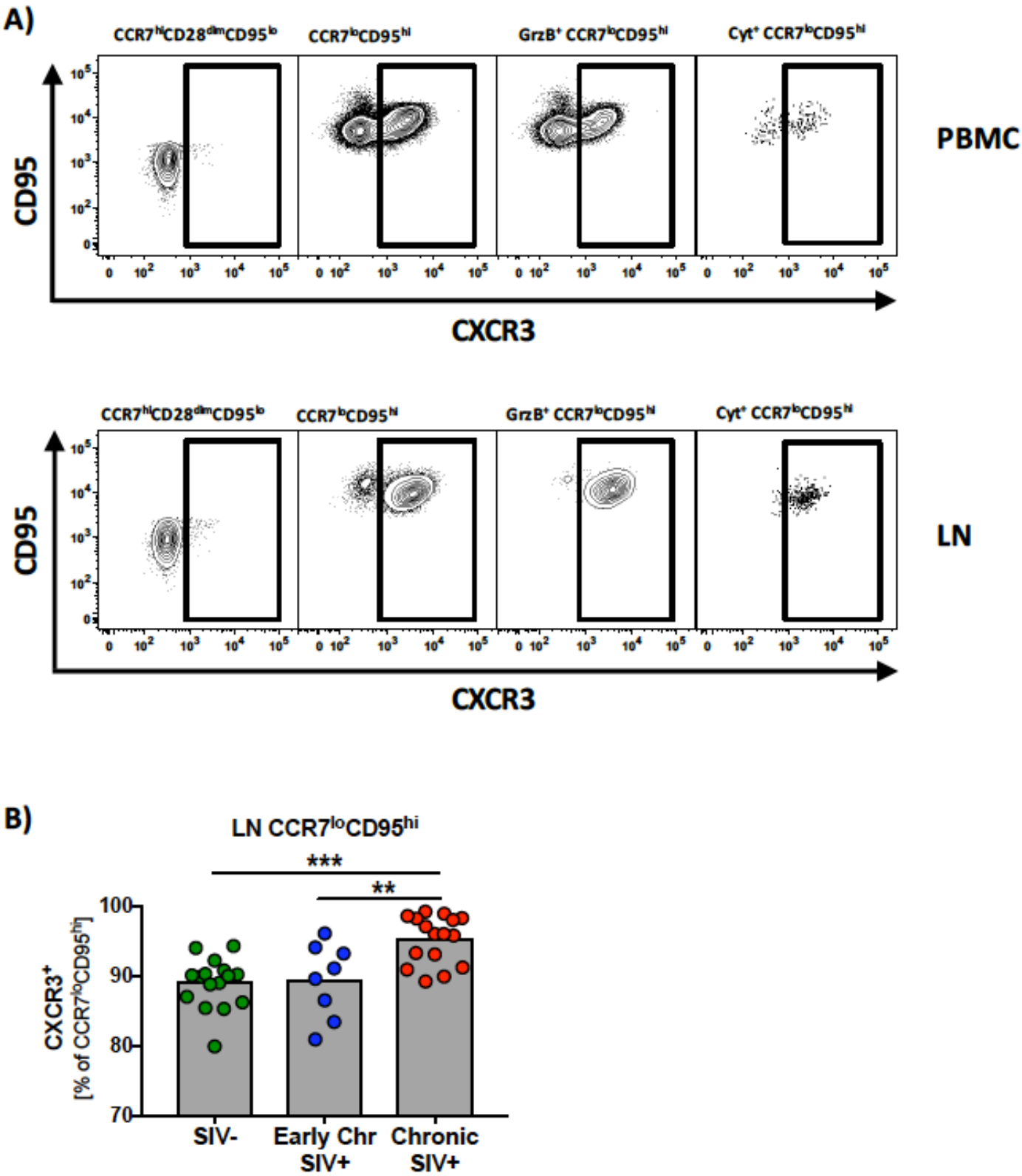

Figure S11. (A) Gating strategy showing the analysis of the CXCR3 expression on different CD8 T cell populations, including cytotoxic CD8 T cells ($GrzB^{+}CCR7^{lo}CD95^{hi}$) and SIV-specific CD8 T cells (Cyt-expressing $CCR7^{lo}CD95^{hi}$). **(B)** Pooled data showing the CXCR3 expression on LN $CCR7^{lo}CD95^{hi}$ CD8 T cells from noninfected, early (d45) and chronic (> 6 months) SIV infected RMs. Results are shown as frequency of the parental. **$p < 0.001$; ***$p < 0.0001$. Mann-Whitney U test for unpaired comparisons.